Copy No. 13

DEFENCE R&D DÉFENSE

PRELIMINARY RESULTS OF AN ALGORITHM FOR AUTOMATIC DETECTION OF MINELIKE OBJECTS IN SIDESCAN SONAR IMAGES

J.A. Fawcett

DEFENCE RESEARCH ESTABLISHMENT ATLANTIC

Technical Memorandum

DREA TM 2000-013

February 2000

National Defence Défense nationale

Canada

National Defence
Research and Development Branch

Défense nationale
Bureau de recherche et développement

PRELIMINARY RESULTS OF AN ALGORITHM FOR AUTOMATIC DETECTION OF MINE-LIKE OBJECTS IN SIDESCAN SONAR IMAGES

John A. Fawcett

February 2000

Approved by R. Kuwahara: R Kuwahara
Head/ Electromagnetics Section

TECHNICAL MEMORANDUM 2000-013

Defence Research Establishment Atlantic

Centre de Recherches pour la Défense Atlantique

Canada

EXECUTIVE SUMMARY

DREA TM 2000-013

PRELIMINARY RESULTS OF AN ALGORITHM FOR AUTOMATIC DETECTION OF MINE-LIKE OBJECTS IN SIDESCAN SONAR IMAGES

by

John A. Fawcett

INTRODUCTION: The detection of mine-like objects in sidescan imagery is of the utmost importance in route-surveying. A trained operator maybe very skilled in doing this, but for images with many possible targets, a manual detection process can be tedious and time-consuming. Thus, it is important to have computer algorithms which can help the operator. A mine-like image is characterized by an area of highlight, corresponding to strong reflection of the acoustic energy and usually a shadow area corresponding to the object blocking acoustic energy from reaching the seabed behind it. However, if the seabed is lossy, then the shadow region may not be well-defined.

PRINCIPAL RESULTS: In this report we investigate the use of two-dimensional filtering of the sidescan image to provide detections. In particular, filters are described which reflect the generic highlight/shadow structure of a typical mine. This filter is then convolved with the data. Where there is a sufficiently high correlation with the data, a detection is indicated. It is demonstrated that the two-dimensional filtering of an image with filters that reflect the generic highlight/shadow structure of a target can be used to automatically detect mine-like objects in images. Two data sets are considered: the first image contains targets with well-defined highlight and shadow regions, the second image illustrates some of the problems which can often be encountered, the targets have poorly defined shadow regions and the seabed itself has bans of relatively high reflectivity which can interfere with the detection process.

SIGNIFICANCE OF RESULTS: The method described in this report could be utilized as a method for automated target detection in further sidescan sonar image processing development for MCDV and remote minehumting applications.

FUTURE PLANS: There are number of areas of future research for this method: (1) the automated selection of a good detection threshold to maximize the probability of detection while keeping the number of false alarms to an acceptable level (2) the investigation of the optimal way to handle poor shadow environments and spatially varying backgrounds. Finally we would like to investigate the performance of various filters with respect to many images – one way to do this is to implement the algorithm as part of the Sonar Image Processing system (SIPS) at DREA.

PRELIMINARY RESULTS OF AN ALGORITHM FOR AUTOMATIC DETECTION OF MINE-LIKE OBJECTS IN SIDESCAN SONAR IMAGES

John A. Fawcett

Abstract:

In this paper we investigate the detection of possible targets in sidescan sonar images using the two-dimensional convolutions of filters with the sidescan image. The filters are designed to reflect the highlight/shadow features of targets. A high convolution value indicates a possible target. Two data sets, one from the SQS-511 sonar and one from a Klein 5000 sonar towed by an autonomous vehicle are analyzed. The results are encouraging and indicate that this method may provide a robust method for automated target detection.

Résumé :

Ce document traite de la détection de cibles potentielles dans les images de sonar à balayage latéral en utilisant les convolutions bidimensionnelles de filtres avec les images obtenues par balayage latéral. Les filtres sont conçus pour refléter les caractéristiques de lumière et d'ombre des cibles. Une valeur élevée de convolution laisse supposer la présence d'une cible. Deux séries de données, l'une obtenue au moyen du sonar SQS-511 et l'autre, à l'aide du sonar Klein 5000 remorqué par un véhicule autonome, ont fait l'objet d'analyses. Les résultats sont encourageants et laissent croire que cette méthode pourrait constituer un bon moyen de détection automatique des cibles.

102-02590/

Introduction

The detection and classification of targets in sidescan sonar imagery is clearly of fundamental importance in a minehunting system. It is difficult to implement detection and classification algorithms which are superiour to a skilled operator. However, manual detection, feature extraction and classification are time-consuming operations and in environment where there are several mine-like objects to be investigated, automated algorithms are required. These algorithms may be used to either replace the operator or, at least, aid the operator in his/her tasks. In this paper we examine a simple detection algorithm.

In a sidescan sonar image, an object on the seabed is characterized by a highlight region (a group of pixels of high intensity) and a shadow area (a region of below average intensity). The highlight is caused by the backscattering of sonar energy from the object due to specular reflections, edge diffractions, point diffractions, etc. The shadow zone is caused by the object blocking acoustic energy from reaching the seabed behind it. The length of the shadow zone is related to the height profile of the object and the grazing angle of the incident energy. Between the highlight and shadow regions of a target there is often a "transition" zone of intermediate levels of energy.

One can formulate standard energy detectors based upon the highlight alone or shadow detectors based upon areas of low energy. Intuitively, a better detector would be based upon looking for combinations of highlight and shadow, typical of mine-like objects. This is the approach taken by Dobeck et al [1] and which we investigate in this paper. We define a two-dimensional filter composed of a highlight region, a shadow region, and a transition region and correlate this with the sidescan image, looking for high correlation values. In general, different filters might be defined to reflect the different possible mine-shapes and orientations.

We consider 2 data sets below. The first is a sidescan sonar image of a field of mine-sized targets off Esquimalt, B.C. The targets are very obvious and have well-defined highlight and shadow regions. Thus, in this case, there would be no difficulty with manual detection. However, for our numerical experiments we will also add a significant level of noise to the original image. The second set of data is from trials of the Canadian autonomous vehicle, DORADO, with a Klein 5000 Sonar near Brest, France. In this case, the targets are more complicated in shape, the seabed reflectivity is variable (in particular, there are bands of higher reflectivity) and the shadow zones are not nearly as distinct as for the Esquimalt case. Thus this is a more difficult case. We do not know the precise target locations in this case, so that the performance of the detector in terms of true target detections cannot be determined . However, we demonstrate the relative performances of filters which (1) emphasizes both the highlight and shadow regions (2) with less emphasis on the shadow region (3) a small highlight-only filter. As mentioned above the bands of higher amplitude in the sidescan image can potentially be a problem to the detection methods; a possible pre-processing approach to this proble would be to

filter this background out; we show that filtering the image in a wavelet-transform space seems to be promising.

Esquimalt Data

Below in Fig.1 we show a bitmap image from the Esquimalt target array. We also show an enlargement of one of the regions in Fig.2. Here we can see 4 very definite cylinders and a small object which is unknown. This 8-bit data has not been geocoded or slant-

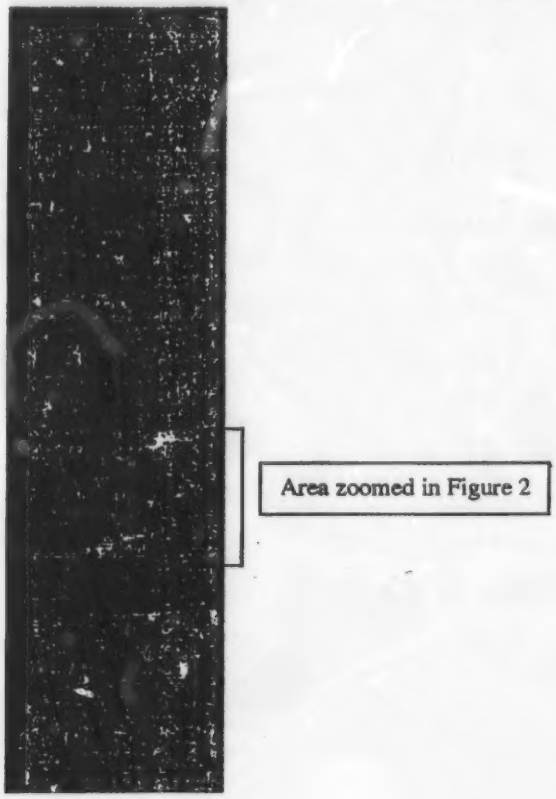

Figure 1. Sidescan image from Esquimalt target array.

range corrected, but the pixel size is approximately 12.5 cm. The data has already had some normalization. In Figure 3 we show a histogram for the full region, the computed mean is 77.61 and the standard deviation is 35.89. We note that because of the compression scheme used, that there are a large number of values in the lowest histogram bin.

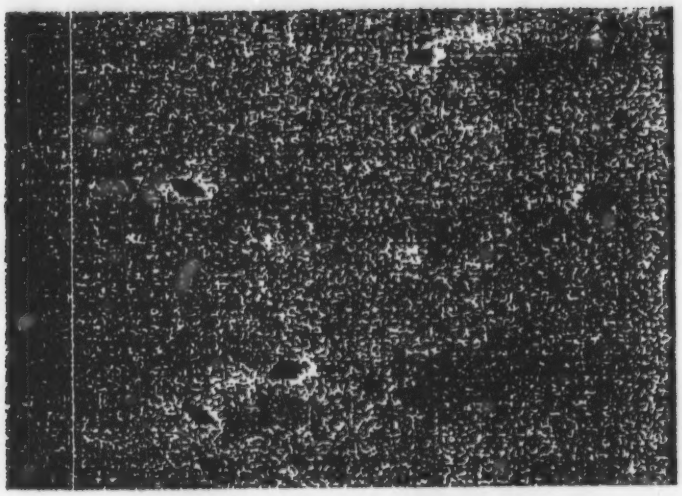

Figure 2. A zoom of a section of Fig. 1

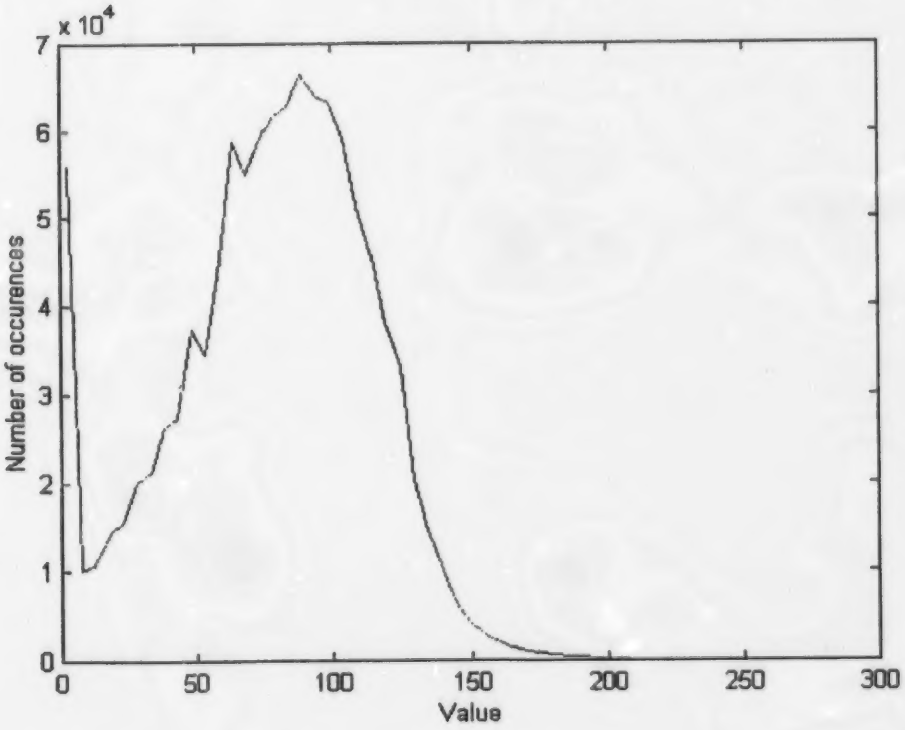

Figure 3. A histogram of the pixel values in the sidescan image

We now subtract the mean from the entire set. The detection algorithm is based upon that suggested by Dobeck et al [1] – namely, we define a mask to reflect the generic highlight/shadow structure of a minelike object. The size of the mask in terms of pixels will vary according to the sonar type. One could also vary the two-dimensional mask to reflect the various typical mine shapes and aspects. In Fig. 4 we show a filter which is designed to simulate a mine which is 75 cm in length (6 pixels); has a highlight region of 75 X 50 cm and a shadow region of 75 cm X 100 cm. For images which are bigger than this, this filter will also detect these objects, but may have multiple detections on the single target. For objects which are smaller than the designed filter, the filter will also often detect these objects, but it is not the optimal matched filter for these detections. In general, one can expect that there will be some mismatch between the filter and the various possible target shapes, orientations, and slant ranges (for data which has not been slant-range corrected). It is, possible to design a suite of filters to reflect the various possible target types, aspects, and geometries. For example, in Fig.5, the same filter as in Fig.4 has been offset one column per row, effectively inclining the filter at 45 degrees. The regions at the beginning and end of the filter are padded with zeros so that the overall mask is still rectangular. This filter would be suited for matching to cylinders at approximately 45 degree aspect.

In the example below, we tried using different masks of different sizes and aspects to see if there was an improvement in detecting certain types of targets and non detecting other types. However, at least for the Esquimalt data, there was no significant advantage in running a suite filters. The zero-aspect mask of Fig. 4, seemed able to detect all the targets, even though there is definitely some mismatch with the sizes and orientations of some of the targets. However, if a filter which is significantly mismatched is used then the performance characteristics do deteriorate, as we shall see below.

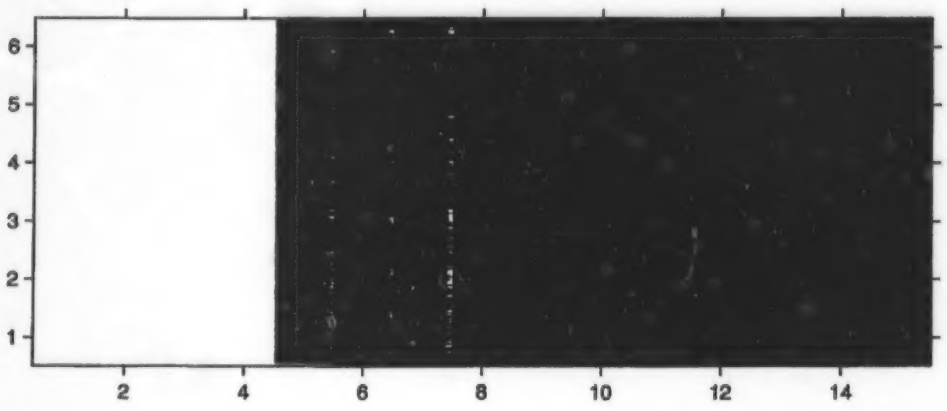

Figure 4 – A mine-like mask for zero aspect – white is +1 and black is -1

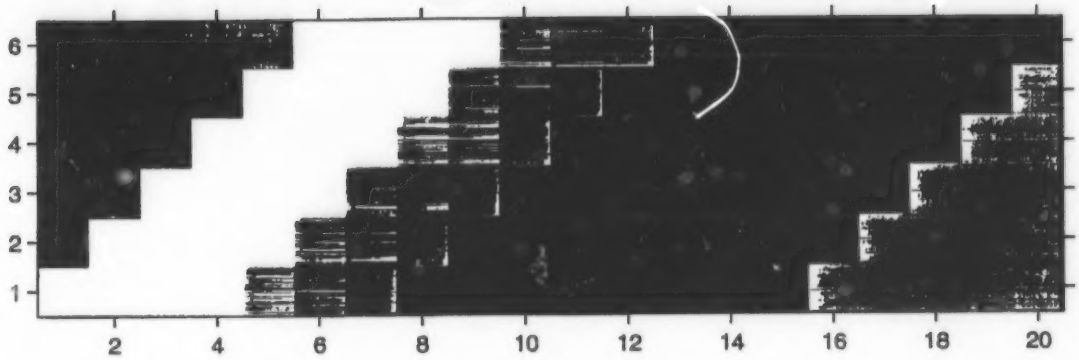

Figure 5 – The same mask as Figure 4 but rotated 45 degrees and with zero-padding at the beginning and end of the mask.

To investigate the ability of the filter of Fig.4 to detect mine-like objects, this filter was convolved two-dimensionally with the Esquimalt data set. High convolution values would then indicate target detections. Our computations were done using MATLAB [2] on a DELL/NT computer – the two-dimensional convolution was carried out using the MATLAB routine (note that the convolution is done with the flipped version of the filter – however for the images concerned, the shadow region is first in terms of the matrix storage so that the filter as defined above is correct). A gray image of the resulting convolved field is shown below in Figure 6. A histogram of the convolved image is given in Fig. 7. As can be seen it looks almost Gaussian, although the distribution is a little asymmetric. There is the question of what value to use for a detection threshhold. If we take the intensities of the original image to be independently distributed random variables with standard deviation 35.89 (as computed from the sidescan image of Fig.1), then an averaged sum of effectively 80 random variables (taking into account the low-weightings of some values of the filter of Fig.4) should have a standard deviation of approximately 324 about the mean of zero. Based upon this one, could choose a threshhold to keep the false alarm rate below some level. However, an empirical computation indicates that the standard devation of the convolved field is, in fact, approximately 453; this is probably due to the fact that the intensities are not independent variables, but in fact there are correlated returns in the image, even for non-target regions. If we set the threshhold level at $2265=5\sigma$, (this gives a Probability of false alarm (Pfa) of 3×10^{-5} % for a Gaussian pdf), we get the detection map of Fig.8. As can be seen these automated detections are in good agreement with the detections that one would make by visual inspection.

If we take a filter which is significantly mismatched in terms of shape of a target then the detection performance does deteriorate somewhat. As an example, consider a 8 X 8 filter

with the first four columns being 1 (highlight) and the last four columns being –1 (shadow). Then the resulting detection map at the 5σ level is shown in Fig. 9. As can be seen all the targets have been detected but there are also some false alarms; raising the detection threshhold eliminates some of the false alarms but also some of the true targets.

In order to make the detection process more challenging, artificial noise is added to the image. In particular, we add squared Gaussian random noise of zero mean and standard deviation of 8; if the noise exceeds 255 it is set to that value. A portion of the noisy sidescan image is shown in Fig.10. The targets are now barely visible to the eye. The resulting convolution image and the detections for a value of 5σ for the filter of Fig.4 are shown in Fig.11. There are the same detections as Fig.8 except for the uppermost target, which is, in fact, a piece of plywood with resolution balls on it.

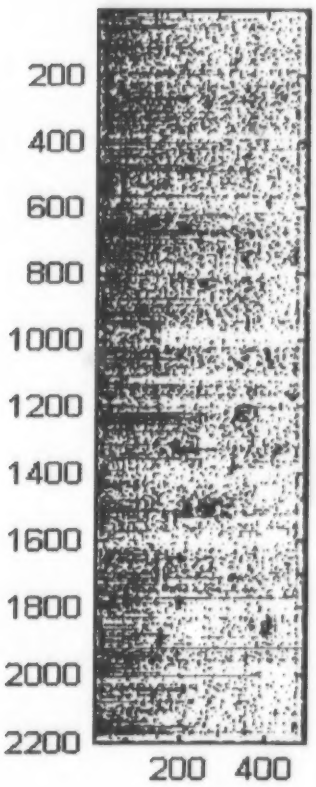

Figure 6. The field resulting from the convolution of the image with the target filter

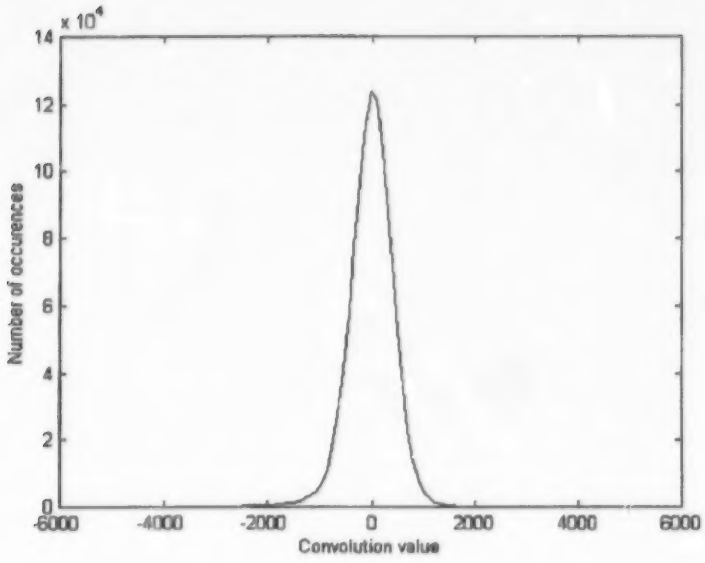

Figure 7. Histogram of pixel values for the convolved field

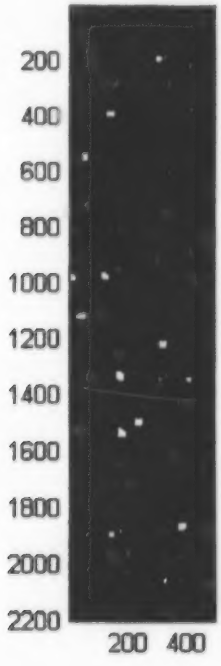

Figure 8. Detections from the convolved field at the 5σ level

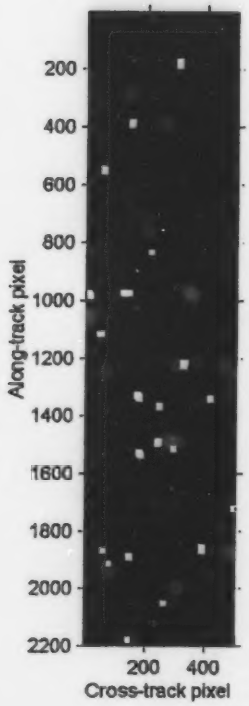

Figure 9. Detections made at the 5σ level for mismatched filter

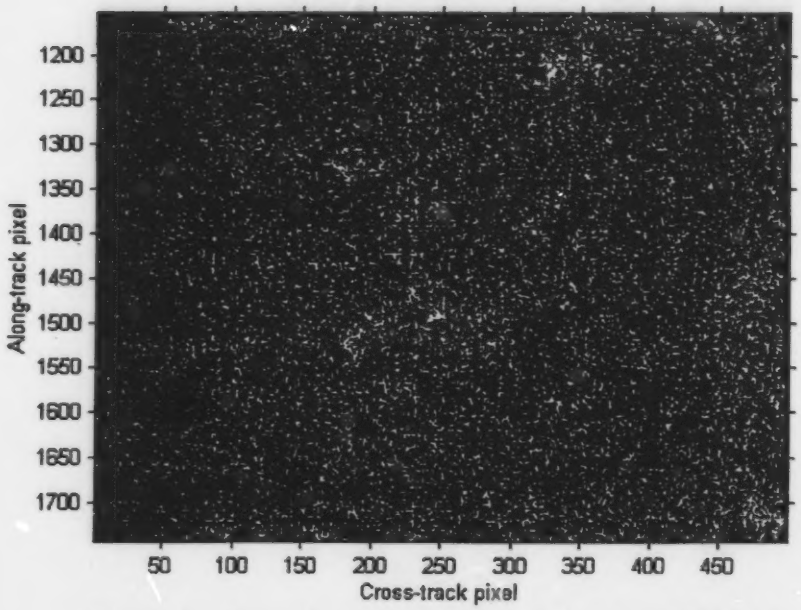

Figure 10. Zoom of sidescan image with noise added to it

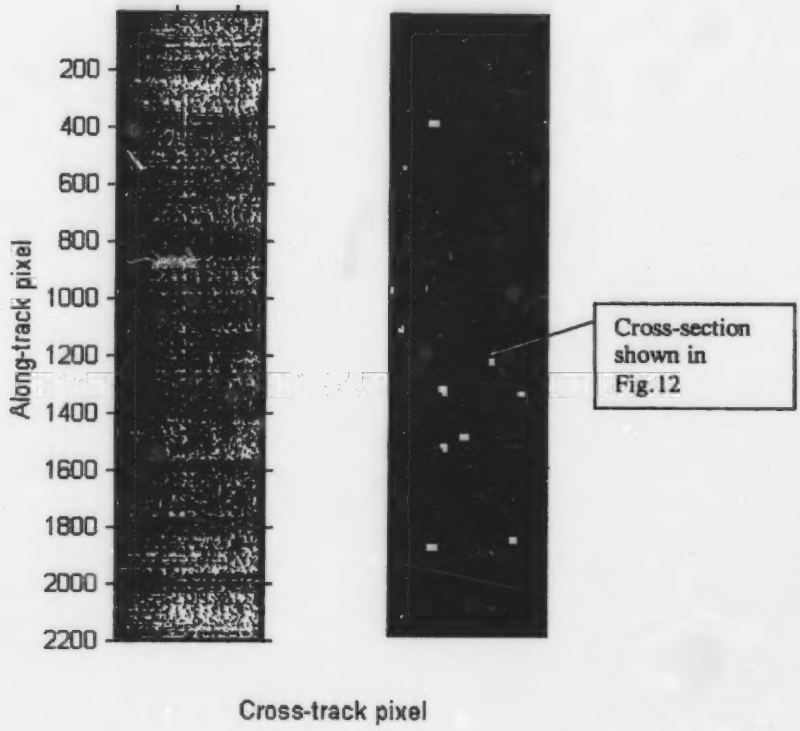

Figure 11. The filtered image and the resulting detections at the 5σ level

We show in Fig. 12, cross-sections through the object indicated above in Fig.11, for the noisy image and the resultant convolved field. Here, the two curves are normalized by their maximum absolute values over the range shown. In the noisy image curve (blue), the object is not apparent with respect to the noisy background; in the convolved (red) curve, the object appears with a much higher peak above the surrounding level.

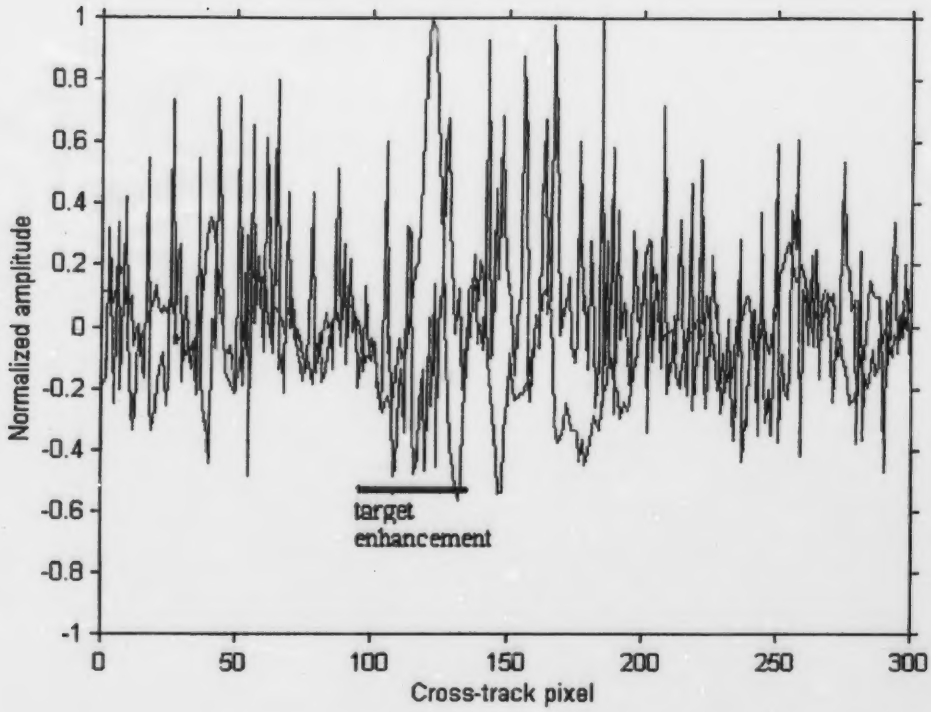

Figure 12. Cross-section at along-track pixel 1200 through noisy image and filtered output for object indicated in Fig.11; Red is the convolved field and blue is the noisy image

French Trial Data

This data set was obtained from a Klein 5500 sonar towed by the DORADO autonomous vehicle. A sequence of targets was laid out along a cable from a release buoy. The raw sidescan image is shown in Fig.13. Bands of high reflectivity in the seabed can be seen. These bands can be a source of false detections. Another very important difference between this set and the previous one is the poor shadow definition.

The release buoy, a portion of the cable, and the sphere are present in Fig.13. There are also other targets, a simulated-Manta,and a cylinder, on the seabed. Unfortunately, the precise locations are not known so that it is not possible to know where in the sidescan image the "mines" are located. The survey was run on a racetrack setup so that the seabed coverage is partially repeated in Fig. 13. A normalization curve is computed by summing along the columns of the pixels and then averaging the results over the number

of rows (along-track pixels). The resulting normalization curve is shown in Fig. 14. The data is then normalized by this curve. The along-track resolution of the sonar is about 20 cm and the across-track resolution is 3 cm. However, this is ungeocoded data and we have used all beams which, in fact, overlap each other , so that there is not a direct conversion between along-track pixel number and position in these figures.

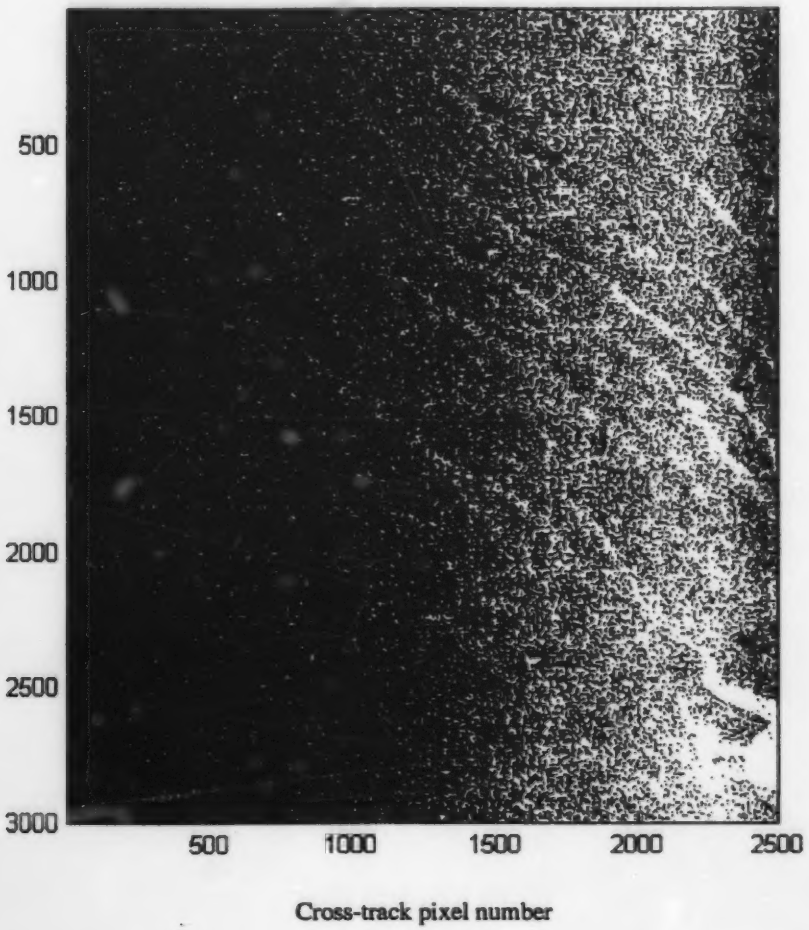

Figure 13 - French Trial data used for analysis – Side scan sonar data from a Klein 5500

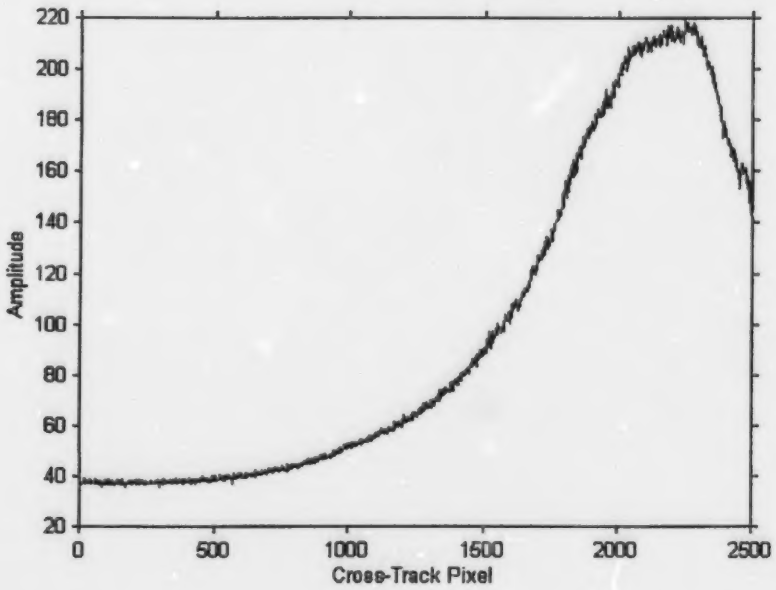

Figure 14. Averaged normalization curve

After normalization by this curve and then subtracting off the mean, the data has the histogram shown in Fig.15. We note that there are 2 peaks in the distribution. The second peak is probably due to the bands of reflectivity in the image. Also the distribution has an extended tail for values greater than two. A section of the normalized image shown in Fig. 15; the values have been clipped at 3.5. In this image the release buoy, a sphere and portions of the connecting cable can be seen.

We now proceed as with the Esquimalt data and define a filter consisting of highlight, a and shadow. In this case the cross-track sampling is about 4 times finer than the previous case so we should make the filter longer in the cross-track dimension. The first filter we consider consists of 6 rows and 10 columns of "1" and 20 columns of - 1 (shadow). The mean is subtracted from the sidescan image set and the resulting image convolved with the filter. The resulting detections at the 5σ level of the convolved field are shown in Fig.16. The detections are all reasonable. For example, in Fig. 17 we show a zoom of the sidescan image near the bottom detection in Fig.16. The detection was on the extended highlight with a weak shadow behind it.

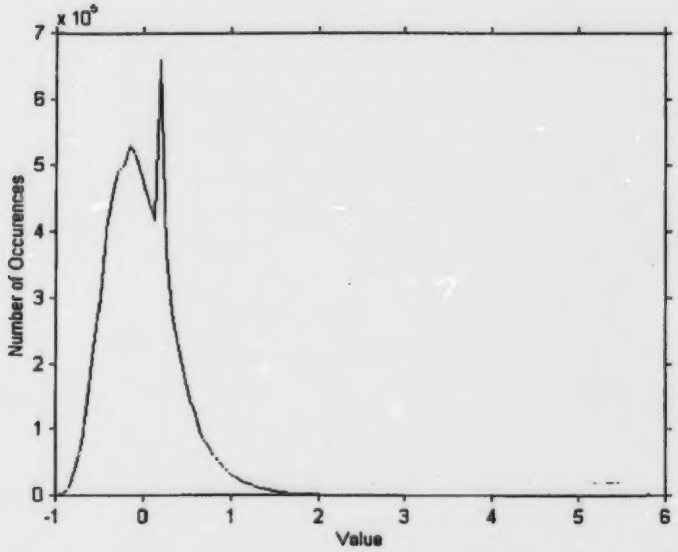

Figure 15. Histogram of normalized image

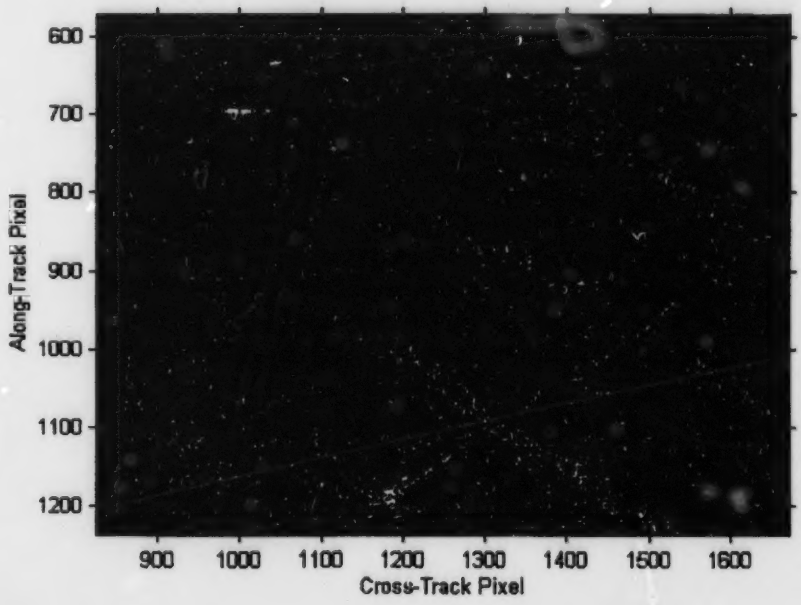

Figure 16. Section of normalized data showing release buoy (1000,700), cable (running diagonally from release), and sphere (1200,1200). Note also the bands in the seabed.

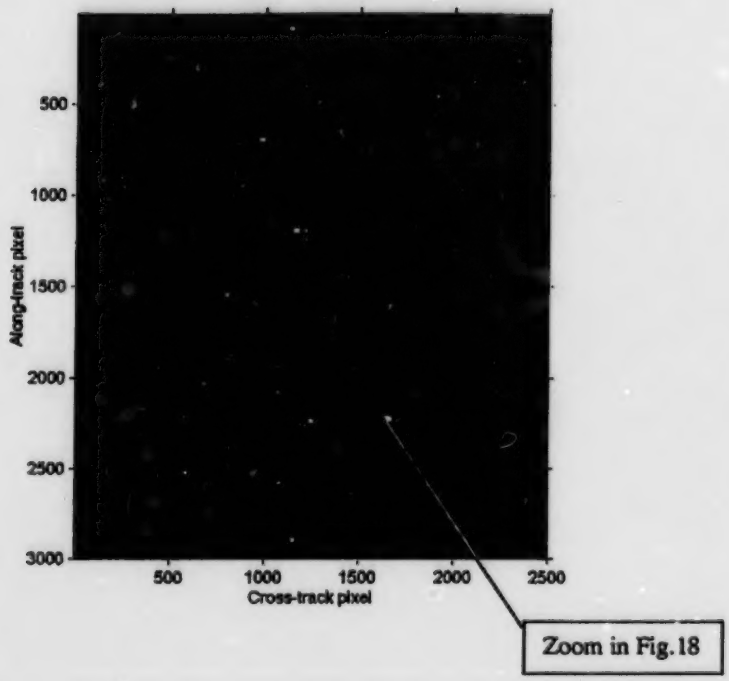

Figure 17. Resulting 5σ detections for the first highlight/shadow filter

This filtering process has identified 7 possible targets. All of these are probably detectable by eye on examination of the original image, although for the object shown in Fig. 18 the filtering has definitely improved the signal-to-noise ratio, as evidenced in the slice through the original, normalized image and the convolution output – Fig.19. In the plots of Fig. 19 we have normalized each curve to have unity maximum absolute value. The convolution curve has a smoother and lower background level. The object is manifested by a significant peak and then a significant trough. The trough is caused by the shadow (-1) region of the filter passing over the highlight region of the object. In fact, since the shadow regions in the sidescan image are so weak in this case, the convolved field will often have a larger minimum than maximum. Another cross-section through the image of a detected object and the corresponding convolution values are shown together in Fig. 20. Here, although there is a peak which is detected the more significant feature is the trough. This is due to the fact that the filter has a large portion of shadow area and the actual image of the object has very little, if any – the negative convolution values result from the shadow of the filter overlapping with the highlight of the object. Also, it is important to note that because of the extent of the filter and the definition of the convolution, the peak of the convolved field will, in general, be offset from the highlight of the original image.

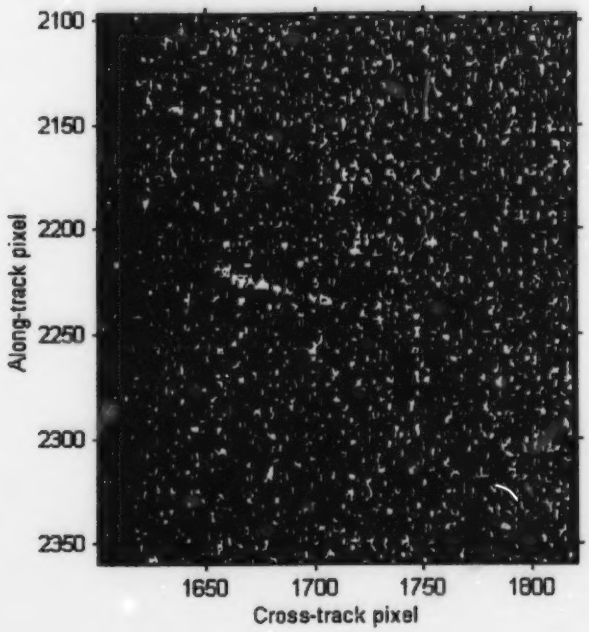

Figure 18 – Section of original data showing an object on the seabed

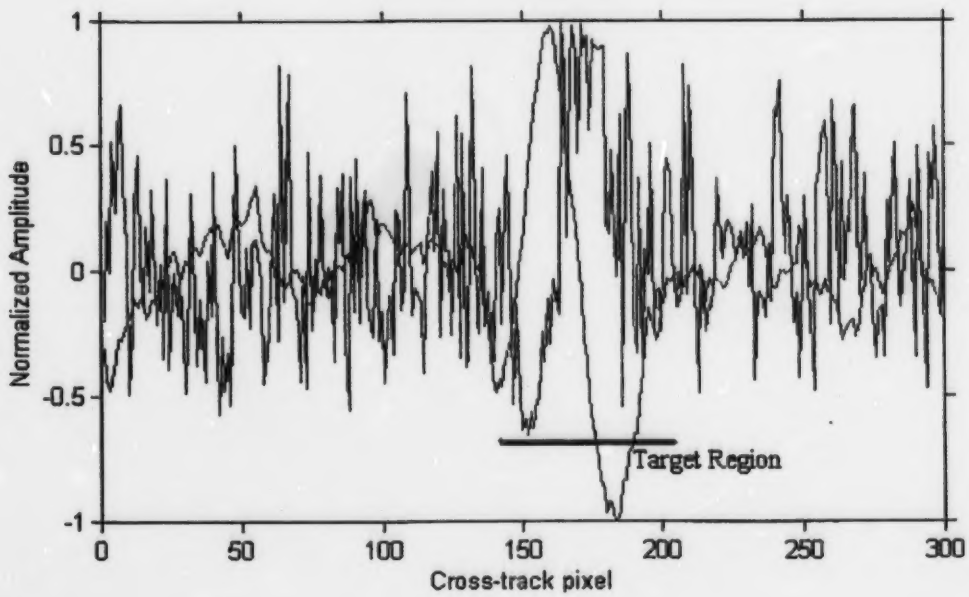

Figure 19. Original image (blue) and filtered result (red) for a slice through object of Fig. 18

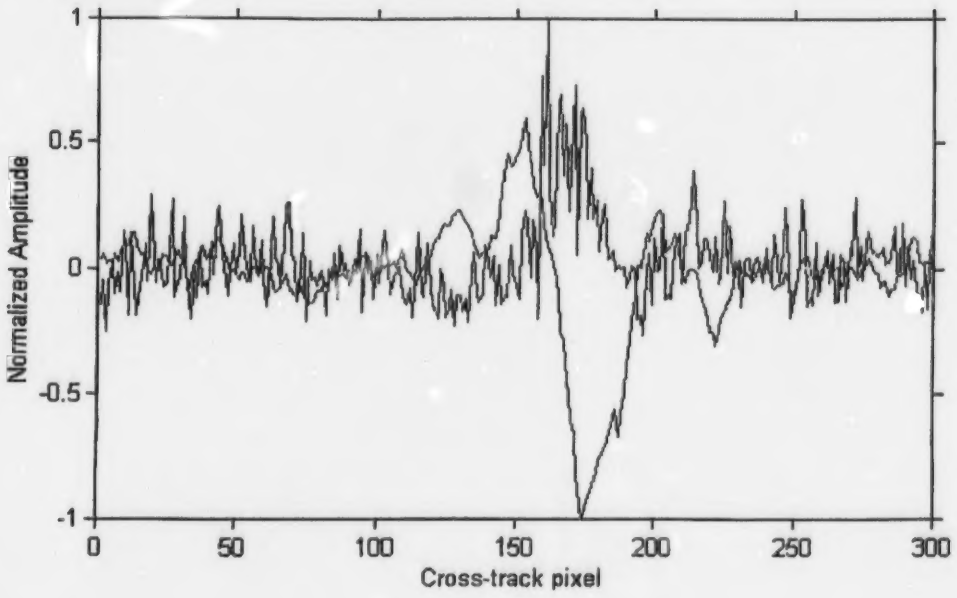

Figure 20. Original (blue) and filtered (red) image for a slice through a stronger-highlight object

Since the original image does not, in general, have good shadow definition it seems reasonable to de-emphasize the shadow portion of the filter. We do this by changing the values of –1 to –0.5 in the filter. In fact, since there are ten columns of highlight and twenty of shadow, these individual weights give equal overall weighting to the highlight and shadow regions. The resulting 5σ detections are shown below in Fig.21.
As can be seen, there are significantly more (in fact, too many) detections using this modified filter. This is because the highlight portion of the filter is now relatively more important and areas of the image with higher amplitudes, such as the bands of sand, are now sufficient to cause detections. One way to improve this situation is to normalize the convolved field with a moving average of the background levels. In particular we take the image, square it element-by-element, and convolve this matrix with a 50X50 filter of ones yielding a moving 50 X 50 average of the background power. The square root of this power is then taken. It should be noted that because of the large size of the filter used, the convolution is rather time-consuming in this case. Normalizing the convolution of the image with this averaged power and then taking the 5σ detections yield the detection map of Fig.22. This seems a much more reasonable detection map – note that there are some double detections on the same object. There are also some additional detections beyond the original detections made in Fig.17. For example, in Fig.23 we zoom in on one of the new detected objects; it would seem to be a reasonable detection. In Fig.24 we show a profile through this object and also the convolved output. For the convolved field there is a peak at the correct location (note that there is an offset due to the length of the filter) but that the background convolved field is somewhat oscillatory indicating that there is still some structure to the background image.

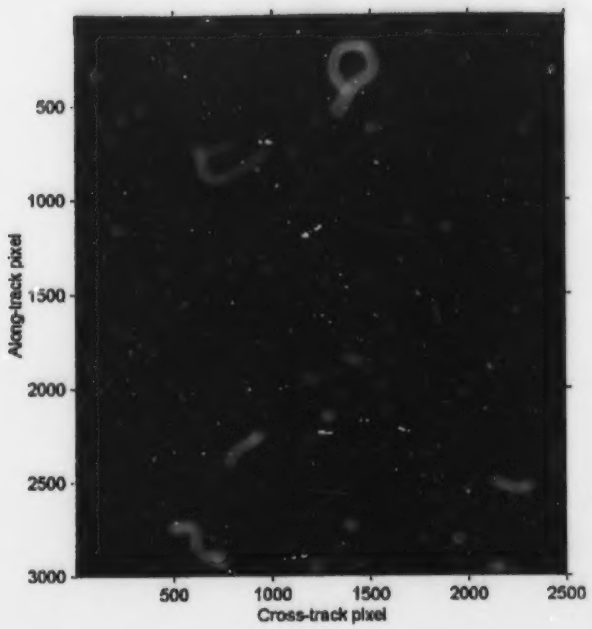

Figure 21 – Resulting 5σ detections using the filter with lesser weighting on the shadow region.

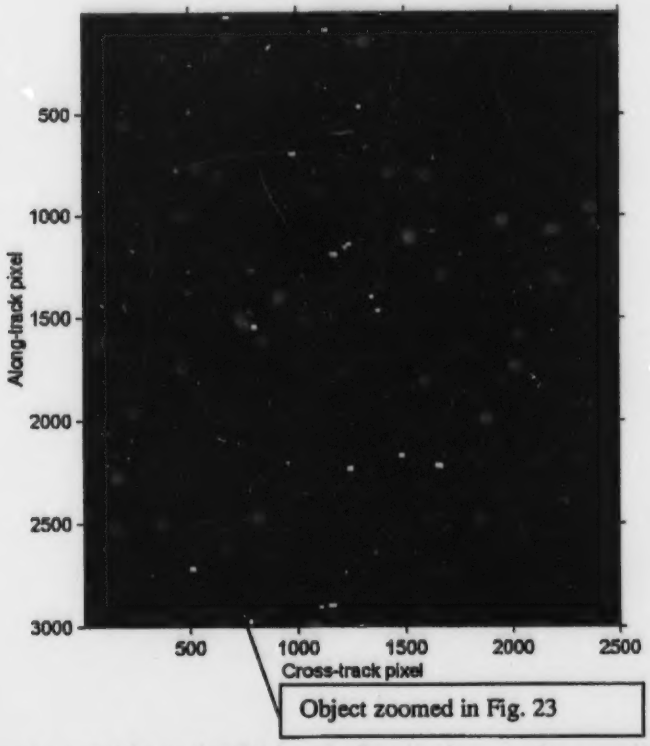

Figure 22. Detections made at the 5σ level after background normalization

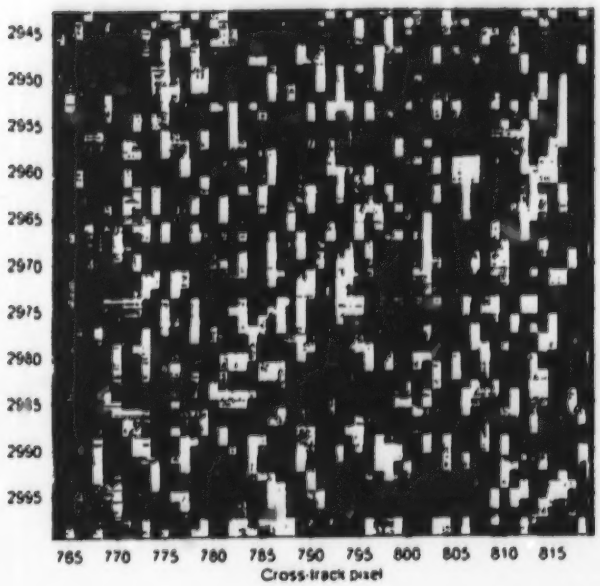

Figure 23. A zoom of the sidescan image about one of the new detections

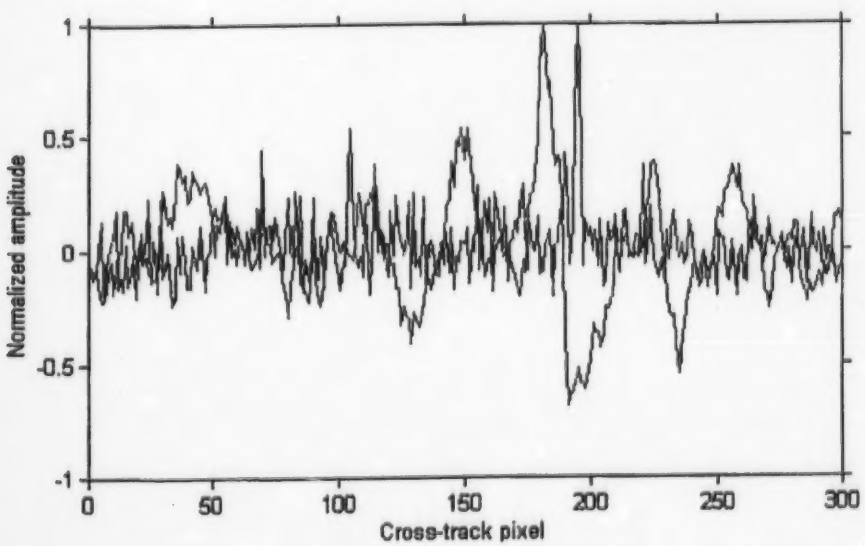

Figure 24. The cross-section through the image (blue) and the convolved field values (red) of the object of Fig. 23

Finally we consider ignoring the shadow regions completely and using only a highlight detector; in particular we use a 6 X 6 filter totally composed of ones. The resulting detections at the 5σ (after normalization by the background intensity) are shown in Fig. 25. There are few new additional detections from the previous filter but not an inordinate number.

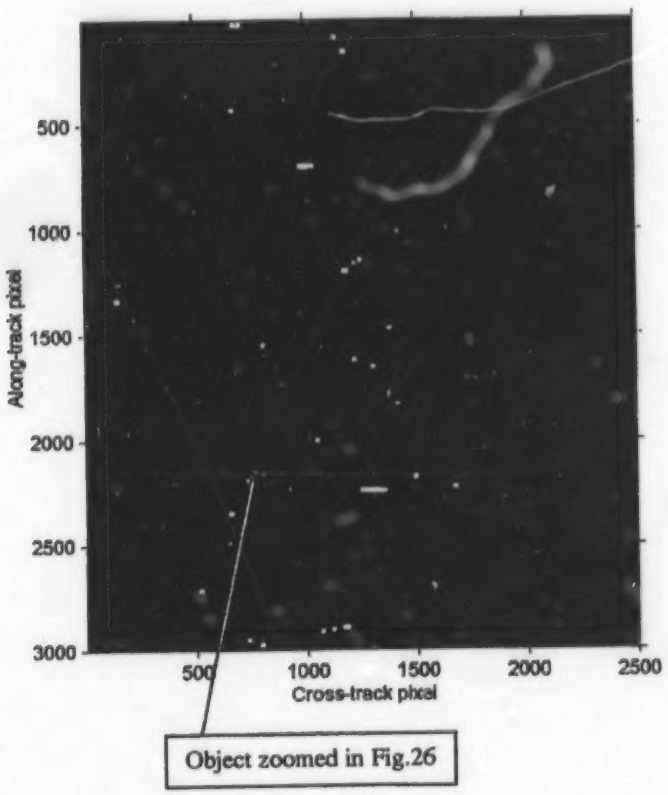

Figure 25. Detections made at the 5σ level for the 6X6 highlight detector

We show in detail in Fig.22 one of the new detections. As can be seen it is rather small and seems to be at the threshhold of being an acceptable detection. In Fig. 23 we show a slice through this object with both the image and convolved fields. As can be seen from this figure there is definitely a highlight where the object is; the filtered output retains the highlight but has a smoothed background level.

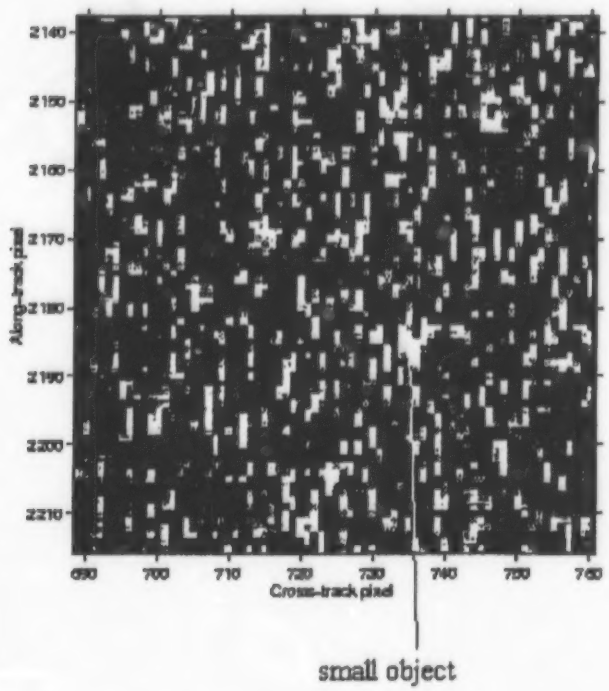

Figure 26. A zoom of one of the new detections

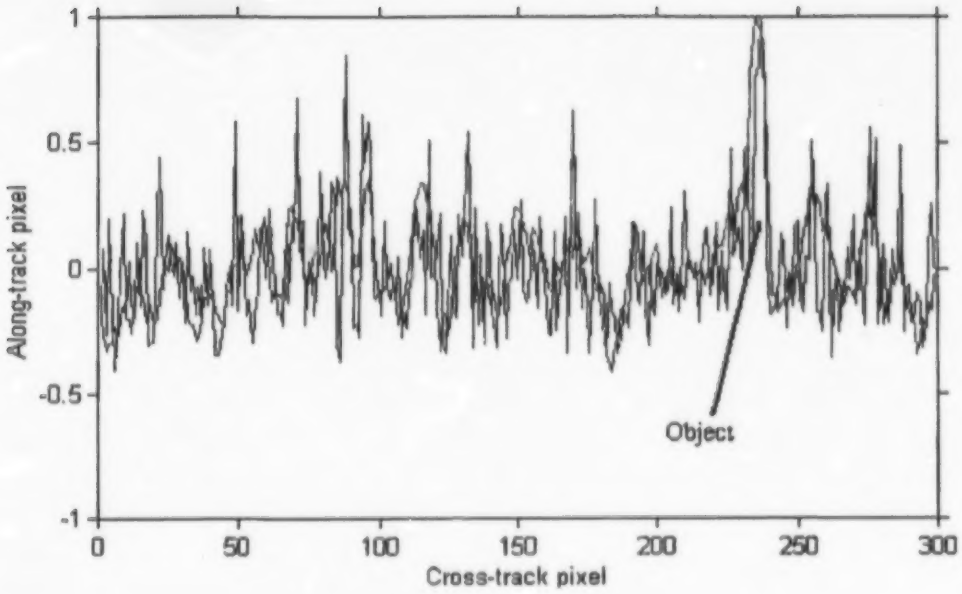

Figure 27. A slice through the object (blue) and the filtered output (red)

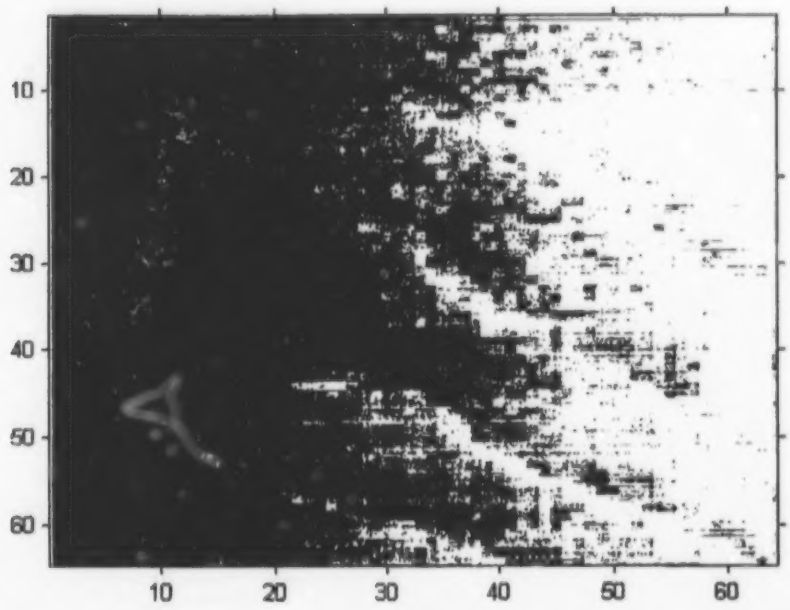

Figure 28 – The "remainder" panel from the two-dimensional wavelet transform of the unnormalized image

This data set is interesting because of (1) its poor shadow definition and (2) its non-uniform background. In particular there is the presence of the bands of relatively high reflectivity (sand) which can cause spurious detections. It was found to be necessary for the last two filtering schemes considered to normalize the filter results by the average background level in order to mitigate this effect. The computation of this running background level is, in fact, computationally expensive (at least with the MATLAB implementation we used). Another possible approach would be to try to prefilter the image to eliminate the banded structure. We considered a 1024 X 1024 section of the top portion of the image. Taking the two-dimensional FFT of the data and examining the resulting two-dimensional spectrum did not indicate any obvious peak in wavenumber space which could be filtered out. However, in Fig. 28 we show the remaining low-"frequency" wavelet coefficients of a two-dimensional wavelet (we used the Haar wavelet as the mother wavelet) transform of the image [3]. The image we use is the "raw" image; the image before even the basic cross-track normalization has been applied. As can be seen much of the varying background is captured in these coefficients; also a portion of the strong release-buoy image is contained in these coefficients. We simply zero this portion of the two-dimensional wavelet coefficients and then invert the result to obtain the image of Fig.29. It can be seen that the bands have to a large degree been eliminated; as well, some of the normalization has been taken care of. However, although the mean of the image has been effectively subtracted out, the absolute values (or standard deviation) does increase towards the right of the image. We compute the average cross-track absolute value and normalize the image and then use the 6 X 6 highlight filter; we do not perform a moving average of the background levels. In Fig. 30 we show the resulting detections made at the 6σ level. At the 5σ level used previously, there are significantly too many detections; it seems that in this case 5σ is just near the border of providing good detection/false alarm characteristics. Wavelet prefiltering has also been applied by other researchers [4]. This seems to be a promising approach to filtering out the varying background features of the sidescan image. However, further research is required into how to optimally do this and the subsequent effect of this filtering on the detection process.

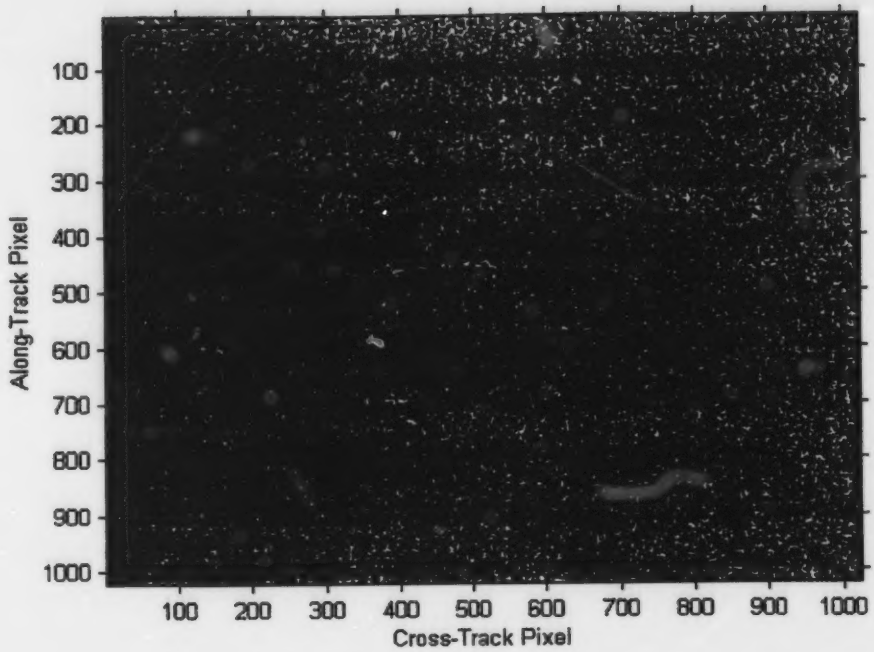

Figure 29. The image resulting from the inversion of the filtered wavelet spectra.

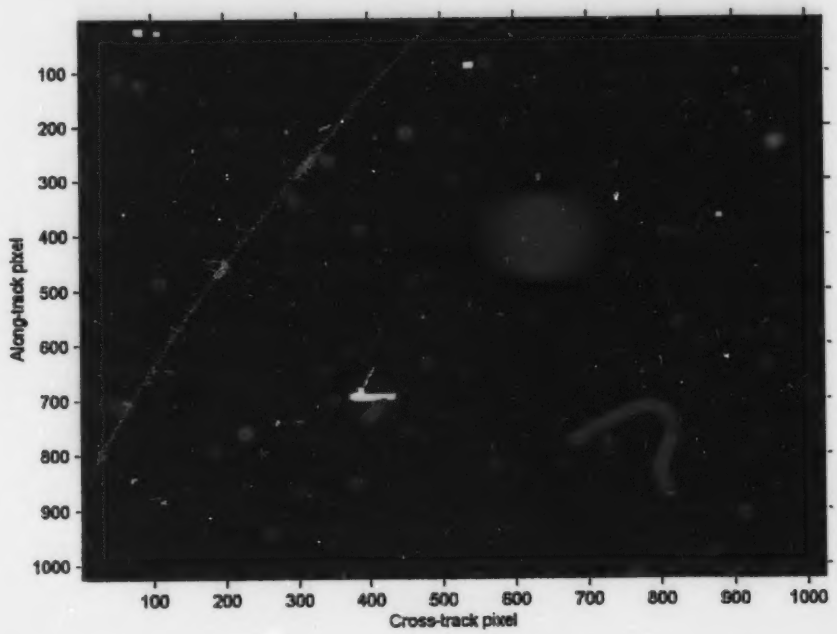

Figure 30. Detections made at the 6σ level

Summary and discussion of results.

We have approached detection from the point of view of a simple convolution of a generic mine image, consisting of highlight and shadow, with a sidescan sonar image. These convolutions can be implemented efficiently and we used a MATLAB routine to do this. In the case of the sidescan imagery from Esquimalt the targets were clear and usually had well-defined shadows; the convolution approach worked very well for the true imagery and with significant noise added. It was seen that the SNR of an object was significantly higher for the filtered field. It was found that by computing the standard deviation of the convolved field, and setting the detection level at 5σ gave excellent results. For the noisy image, it was seen that the detection performance was dependant upon choosing a good filter. However, when a filter was used which was significantly mismatched to the highlight/shadow structure of a mine-like object, the detection performance did deteriorate.

We then considered a data set from a Klein 5000 sonar towed by the semi-submersible ROV, DORADO, from its trials off Brest, France. This data set illustrated problems for detection that were not evident in the Esquimalt data set. First, there was poor shadow definition. Some of the objects did have a shadow and a filter with a highlight region and a large shadow area succeeded in detecting some objects which clearly were acceptable detections. However, there were "objects" which did not have much shadow but had significant highlight and were not detected by this filter. Because of this we tried two other filters, one which weighted the shadow region less and one which was only a highlight detector. These filters were affected by another feature of this imagery, the inhomogeneous background, in particular, the bands of higher reflectivity. In order, that these bands did not become a multitude of "detections" the filtered image had to be normalized by a moving estimate of the local background level.

Finally, we showed that prefiltering the image by using a two-dimensional wavelet transform and filtering out the low-order wavelet coefficients seemed to effectively reduce the background variations of the image. This is a technique which deserves further study.

One problem for the detection scheme outlined in this report is the setting of threshhold levels for detection. In this report we simply set the level to five or six standard deviations of the filtered field levels. This seemed to give reasonable detections. However, in general, it is not clear how to automatically set this threshhold. It may be that in some cases this level will produce too many false alarms; on the other hand one would prefer some false detections, which might be ruled out by susbsequent analysis, rather than missed mines.

Also, in the 2 cases considered in this report the objects detected were fairly isolated from each other; the performance of these highlight/shadow detectors might deteriorate in a clutter area.

In future, we would like to implement some of these filters in the SIPS computer system and evaluate their performance on data sets as they are processed.

References

1. G.J. Dobeck, J.C. Hyland, and Le'Derick Smedley, "Automated detection/classification of sea mines in imagery" obtained from http://www.ncsc.navy.mil/CSS/Papers/SonarImagery/paper.htm

2. *MATLAB The Language of Technical Computing, Using MATLAB Version 5*, The Mathworks Inc. , January 1997.

3. J. Buckheit, S. Chen, D. Donoho, I. Johnstone, J. Scargle, "WaveLab .701", http://www-stat.stanford.edu/~wavelab/

4. Q. Hunyh, N. Neretti, N. Intrator, and G. Dobeck, "Image enhancement for pattern recognition", SPIE Proceedings, Vol. 3392.

UNCLASSIFIED
SECURITY CLASSIFICATION OF FORM
(highest classification of Title, Abstract, Keywords)

DOCUMENT CONTROL DATA

(Security classification of title, body of abstract and indexing annotation must be entered when the overall document is classified)

1. ORIGINATOR (the name and address of the organization preparing the document.. Organizations for whom the document was prepared, e.g. Establishment sponsoring a contractor's report, or tasking agency, are entered in section 8.)

Defence Research Establishment Atlantic
PO Box 1012
Dartmouth, Nova Scotia, Canada B2Y 3Z7

2. SECURITY CLASSIFICATION (overall security classification of the document including special warning terms if applicable).

UNCLASSIFIED

3. TITLE (the complete document title as indicated on the title page. Its classification should be indicated by the appropriate abbreviation (S,C,R or U) in parentheses after the title).

Preliminary results of an algorithm for automatic detection of mine-like objects in sidescan sonar images

4. AUTHORS (Last name, first name, middle initial. If military, show rank, e.g. Doe, Maj. John E.)

John A. Fawcett

5. DATE OF PUBLICATION (month and year of publication of document)	6a. NO .OF PAGES (total containing information Include Annexes, Appendices, etc).	6b. NO. OF REFS (total cited in document)
February, 2000	28 (approx.)	4

7. DESCRIPTIVE NOTES (the category of the document, e.g. technical report, technical note or memorandum. If appropriate, enter the type of report, e.g. interim, progress, summary, annual or final. Give the inclusive dates when a specific reporting period is covered).

TECHNICAL MEMORANDUM

8. SPONSORING ACTIVITY (the name of the department project office or laboratory sponsoring the research and development. Include address).

Defence Research Establishment Atlantic

9a. PROJECT OR GRANT NO. (if appropriate, the applicable research and development project or grant number under which the document was written. Please specify whether project or grant).	9b. CONTRACT NO. (if appropriate, the applicable number under which the document was written).
Project 1da12	

10a ORIGINATOR'S DOCUMENT NUMBER (the official document number by which the document is identified by the originating activity. This number must be unique to this document.)	10b OTHER DOCUMENT NOs. (Any other numbers which may be assigned this document either by the originator or by the sponsor.)
DREA TM 2000-013	

11. DOCUMENT AVAILABILITY (any limitations on further dissemination of the document, other than those imposed by security classification)

(X) Unlimited distribution
( ) Defence departments and defence contractors; further distribution only as approved
( ) Defence departments and Canadian defence contractors; further distribution only as approved
( ) Government departments and agencies; further distribution only as approved
( ) Defence departments; further distribution only as approved
( ) Other (please specify):

12. DOCUMENT ANNOUNCEMENT (any limitation to the bibliographic announcement of this document. This will normally correspond to the Document Availability (11). However, where further distribution (beyond the audience specified in (11) is possible, a wider announcement audience may be selected).

UNCLASSIFIED
SECURITY CLASSIFICATION OF FORM

13. ABSTRACT (a brief and factual summary of the document. It may also appear elsewhere in the body of the document itself. It is highly desirable that the abstract of classified documents be unclassified. Each paragraph of the abstract shall begin with an indication of the security classification of the information in the paragraph (unless the document itself is unclassified) represented as (S), (C), (R), or (U). It is not necessary to include here abstracts in both official languages unless the text is bilingual).

In this paper the detection of possible targets in sidescan sonar images using two-dimensional convolutions of filters with the sidescan image is investigated. The filters are designed to reflect the highlight/shadow features of targets. A high convolution value indicates a possible target. Two data sets, one from the SQS-511 sonar and one from a Klein 5000 sonar towed by an autonomous vehicle are analyzed. The results are encouraging and indicate that this method may provide a robust method for automated target detection.

14. KEYWORDS, DESCRIPTORS or IDENTIFIERS (technically meaningful terms or short phrases that characterize a document and could be helpful in cataloguing the document. They should be selected so that no security classification is required. Identifiers, such as equipment model designation, trade name, military project code name, geographic location may also be included. If possible keywords should be selected from a published thesaurus. e.g. Thesaurus of Engineering and Scientific Terms (TEST) and that thesaurus-identified. If it not possible to select indexing terms which are Unclassified, the classification of each should be indicated as with the title).

Detection, filters, convolution